Microbial diversity decline and community response are decoupled from increased respiration in warmed tropical forest soil

Title: Microbial diversity and community response are decoupled from increased respiration in warmed tropical forest soil

Authors: Andrew T. Nottingham[1,2,3*], Jarrod J. Scott[3], Kristin Saltonstall[3], Kirk Broders[3,4], Maria Montero-Sanchez[3], Johann Püspök[3], Erland Bååth[5], Patrick Meir[2,6]

Affiliations:

[1]*School of Geography, University of Leeds, Leeds, UK*

[2]*School of Geosciences, University of Edinburgh, Crew Building, Kings Buildings, Edinburgh, UK*

[3]*Smithsonian Tropical Research Institute, 0843-03092, Balboa, Ancon, Republic of Panama*

[4]*USDA, Agricultural Research Service, National Center for Agricultural Utilization Research, Mycotoxin Prevention and Applied Microbiology Research Unit. Peoria, IL. 61604, USA*

[5]*Section of Microbial Ecology, Department of Biology, Lund University, 22362, Lund, Sweden.*

[6]*Research School of Biology, Australian National University, Canberra, ACT 2601, Australia*

**Corresponding author. Email: A.Nottingham@leeds.ac.uk*

Soil microbes form some of the most diverse biological communities on Earth and are fundamental in regulating the terrestrial carbon cycle. Their response to climate warming could therefore have major consequences for future climate, particularly in tropical forests where high biological diversity coincides with a vast store of soil carbon. Here, we show high sensitivity of the tropical forest soil microbial community and growth to two-years of *in situ* soil warming, which was decoupled from large increases in CO_2 emission. Microbial diversity declined markedly, especially of bacteria. As the microbial community composition shifted under warming, many taxa were no longer detected and others, including taxa associated with thermophilic traits, were enriched. This community shift resulted in an adaptation of growth to warmer temperatures, which we used to specify a microbial model to predict changes in soil CO_2 emissions. However, the observed *in situ* CO_2 emissions increase exceeded the rates predicted by our model three-fold. The additional emissions were driven by acceleration of enzymatic activity, likely through abiotic processes because activity increased even at temperatures beyond the optimal temperature for microbial growth. Our results suggest that warming of tropical forests will have rapid, detrimental consequences both for soil microbial biodiversity and future climate.

Microbial communities sustain the biosphere by cycling carbon (C) and nutrients between the Earth and the atmosphere. As a result, their response to warming provides a fundamental feedback on the terrestrial C cycle and climate, and will have direct consequences for the function and maintenance of terrestrial biota[1]. The nature of this feedback is especially critical for tropical forests, because they exchange more carbon dioxide (CO_2) with the atmosphere than any other ecosystem, contain over a third of global soil C[2], two-thirds of terrestrial plant biomass[3], and represent the apex of global terrestrial biodiversity[4]. Under current emission scenarios, temperatures in the tropics are predicted to warm by 2-5°C by 2100[5] and to exceed historical precedent more quickly than anywhere else on Earth[6]. Despite this, we have almost no information on the magnitude and direction of soil microbial feedbacks under warming for the huge C stores and biodiversity found in tropical forests[7].

Climate warming is predicted to increase soil C mineralisation and CO_2 emission from soil to the atmosphere[8]. Numerous experiments performed outside the tropics have shown that warming increases CO_2 emission from soil[9], and that changes in the microbial community composition and activity determine the associated soil C loss[10,11]. In tropical forests where soils contribute a major portion of these ecosystems' globally significant total C exchange with the atmosphere[12], small fractional increases in CO_2 emission from soils will have a large impact on the atmosphere and climate. Warming experiments in tropical forests have only recently been initiated and first results point towards a large response. Two years of *in situ* full-profile soil warming by an average 4°C increased the soil CO_2 efflux by 55% for a tropical forest in Panama[13], and significantly for a tropical forest in Puerto Rico under infra-red soil warming by 4°C (Wood et al, pers. com.)[*]. These results provoke key fundamental questions: what are the drivers of the large CO_2 emissions from warmed tropical forest soils – and are

[*] Prior to publication, we will amend this line to include detail on the % increase and include the full citation of the paper from this Puerto Rico experiment (the authors understand the results are currently in review/press)

78 they related to abiotic or biotic process, including changes in the composition of the microbial
79 community, its diversity and/or its activity, as found in other ecosystems[10,11,14].
80
81 The response of soil C to warming is underpinned by changes in soil microbial activity, via the
82 instantaneous sensitivity of microbial growth and respiration, which can be modified over time by
83 adaptive change in the microbial community composition[10,15]. These microbial responses have been
84 represented in models of soil C temperature sensitivity by the efficiency of growth and respiration[16],
85 while the thermal response of growth and respiration has been described by the square root model[15,17].
86 In the square root model, the moderating effect of temperature adaptation is described by a change in
87 the theoretical value of T_{min} (the minimum temperature for growth), corroborated by observations that
88 T_{min} is strongly correlated to mean annual temperature differences across climatic gradients globally[18-
89 20]. For example, T_{min} for bacterial growth ranges from approximately -15ºC in arctic ecosystems to
90 approximately 0ºC for tropical ecosystems, with similar patterns observed for T_{opt}[15,19] and for
91 respiration[20]. Across temperate temperature ranges, T_{min} has been observed to increase under
92 experimental warming[21,22] alongside community compositional shifts[14,23,24], thus indicating that the
93 observed thermal adaptation occurred via microbial community composition change. Despite the
94 proven importance of this relationship in determining the temperature response of activity and its
95 thermal adaptation[15,17], we have no information on whether it holds under warming in the lowland
96 tropics, where the mean annual temperature is already close to the predicted optima for activity[15].
97
98 The effect of warming on tropical forest soil C will depend not only on the response of the soil
99 microbial community activity[7], but also its community composition and diversity, which may have
100 consequences for other biota[25]. In a temperate forest, two decades of experimental warming increased
101 bacterial diversity,[14] specifically for lignin-degrading microbes[26]; this positive temperature-diversity
102 relationship is consistent with observations across natural temperature gradients where soil pH and

103 moisture are held constant[23,27,28]. It is unknown whether soil microbial diversity will similarly increase
104 under the novel high-temperature regimes predicted for the tropics[6] and will depend on the thermal
105 tolerance of the microbial taxa present[24,29]. Nor is it understood how diversity change would affect soil
106 process rates, although the effect might be considerable given phylogenetic evidence for high niche
107 specialization among tropical forest microbial taxa[30]. The historically-novel high temperature regimes
108 predicted for the tropics this century[6] (e.g. 2-5°C atmospheric warming[5] added to 1-3°C warming
109 through land-use change and reduced transpiration[31]) could result in temperature maxima that exceed
110 a metabolic threshold for portions of the tropical forest soil microbial community, with potentially
111 large implications for ecosystem functioning and the climate.
112
113 Here we used an *in situ* warming experiment to test the response of the soil microbial community, and
114 its growth and respiration to warming over a range of 3 to 8°C above ambient – thereby providing the
115 first test of how tropical forest soil communities and function respond across these levels of warming
116 in a field experiment. The experiment, SWELTR (Soil Warming Experiment in Lowland TRopical
117 forest) consists of five pairs of circular control and warmed plots (whole-profile warming, using buried
118 resistance cables) distributed evenly within approximately 1 ha of semi-deciduous moist lowland
119 tropical forest on Barro Colorado Island, Panama[13]. Each warmed plot has a ground surface area of
120 ~20 m^2 and is heated across the full soil profile, resulting in a total of 120 m^3 of warmed soil for the
121 experiment. For this study we established two subplots per treatment plot that differed with distance
122 to the heating source, thus providing two treatments of, on average, 3°C and 8°C warming of surface
123 soils (0–20 cm depth). Two years after the warming treatment was initiated, we conducted field
124 campaigns during the wet season (when moisture was non-limiting) to measure soil CO_2 efflux, to
125 characterise the temperature sensitivity of instantaneous microbial growth, respiration and enzyme
126 activities, and to determine the microbial community composition. We tested the hypotheses that: (1)
127 warming will change the α-diversity and community composition of soil bacteria and fungi; (2) the

128 temperature sensitivity of microbial communities (with respect to growth, T_{min}, and enzymatic activity)
129 will become 'adapted' to the new temperature regime (whether adaptation is via genetic change within
130 species, phenotypic plasticity or community-composition change, *sensu* Pietikäinen et al.; Bradford
131 [32,33]); and (3) soil CO_2 emission will increase under 3 to 8ºC warming and follow the increase predicted
132 by the temperature sensitivity of microbial growth and respiration.
133
134 Two years of soil warming reduced the diversity of both bacteria and fungi and caused large shifts in
135 the microbial community composition (Fig. 1). The diversity decline was largest for bacteria, occurring
136 via the loss of proportionally-abundant taxa (Shannon and Inverse-Simpson indices declined; Fig. 1,
137 Extended Data Fig. 1). For fungi, our results suggest a diversity decline due to loss of rare taxa (species
138 richness declined but not Shannon and Inverse-Simpson indices), although this result is less definitive
139 that for bacteria, given methodological difficulties when detecting rare taxa (see Supplementary
140 Methods) and our detection of new fungal taxa in warmed soils (see below). Warmed soils also hosted
141 microbial species (defined by Amplicon Sequence Variants, ASVs) that were undetected in soils at
142 ambient temperature, especially among fungi, although the number of newly detected species was too
143 few to offset the number of species no longer detected (Fig. 1). This decline in diversity, especially for
144 the bacteria, may have negative implications for soil functioning, given the prevailing paradigm of a
145 positive relationship between biological diversity and ecosystem functioning[34], also supported for
146 soils[35,36]. Such a decline in soil microbial diversity under warming is also contrary to positive
147 relationships between temperature and diversity observed in a temperate warming experiment[14] and
148 across natural environmental gradients[27,28,37]. This positive relationship is consistent with metabolic
149 theory of ecology (i.e. positive correlation between energy input, evolutionary rates and diversity)[38]
150 and is considered to contribute a positive feedback on tropical plant diversity[39]. [40,41]. Our results point
151 towards a breakdown in this energy-diversity relationship for tropical soil bacterial communities after
152 a two-year period where temperatures ranged from 29–34ºC. These temperatures may represent a

thermal maximum for the persistence of many species, implying that our findings can also provide insight over timescales longer than the duration of our warming treatment.

Warming also caused large shifts in community composition (Figs. 1–2, Extended Data Figs. 1–5), with many taxa significantly increasing or decreasing in relative abundance with warming by 3ºC, and further with warming by 8ºC (Fig. 1; Extended Data Figs. 2–3). In warmed soils there was a decrease in the relative abundance of Bacteroidetes, a common non-spore-forming bacterial group which comprise taxa that are primary degraders of polysaccharides[42]. For fungi, there was decrease in the relative abundance of members of the Basidiomycota including the Agaricales, a broad order of saprophytic fungi, and the ecologically diverse yeast order, Sporidiobolales. In contrast, warming increased the relative abundance of Firmicutes, a diverse and stress-tolerant bacterial phylum, able to form endospores resistant to desiccation and high temperatures[43]. Indeed, taxa within the Firmicutes have been identified as warm-responsive in laboratory studies[24,29] and in field soil warming experiments outside the tropics[14,44]. Warming also increased the abundance of the class Thermoleophilia within the Actinobacteria, known to include aerobic thermophiles[45]. For fungi, warming increased the relative abundance of Glomerales—arbuscular mycorrhizae—as also seen in warming experiments outside the tropics[46]. In addition, warming increased the relative abundance of several orders in the phylum Ascomycota, including the Eurotiales, Hypocreales and Pezizales, which include thermotolerant saprophytic and pathogenic species, as well as saprophytic and pathogenic yeast in the Saccharomycetales. Thus, broadly, changes in diversity under warming occurred alongside shifts in communities towards thermotolerant microorganisms.

Adaptation of the microbial community to warming potentially can have a large influence on long-term change in soil C emissions[10,16]. To assess this, we used laboratory incubations to determine the instantaneous temperature sensitivity of bacterial growth (T_{min})[15,17]. We found T_{min} to increase under

178 3°C warming and to increase further under 8°C warming (Fig. 2); where the observed magnitude of
179 increase in T_{min}, of 0.3°C per 1°C warming, is consistent with observations made elsewhere[15].
180 Furthermore, among all the parameters associated with temperature adaptation in the field experiment,
181 T_{min} was the most significant correlate of the change in bacterial and fungal diversity and community
182 composition (Fig. 2e, Extended Data Tables 1–2). Thus, while acknowledging that we cannot exclude
183 an influence of genetic change within species on this temperature adaptation, our results strongly
184 suggest that adaptation occurred through community compositional change, as found elsewhere[24], and
185 the development of a microbial community functionally adapted to the warmer conditions.
186
187 These changes in diversity and community composition occurred alongside altered soil process rates
188 in the field experiment: increased bacterial growth rates, enzyme activity per unit microbial biomass
189 for 7 hydrolytic and oxidative enzymes involved in C, N and P cycling (although microbial biomass
190 remained stable) and, measured *in situ*, increased soil CO_2 emission (Figs. 2–3, Extended Data Figs.
191 5–6). Soil CO_2 emission in the field experiment increased markedly at warmer temperatures: 78%
192 higher than controls under 3°C warming and 337% higher under 8°C warming of surface soils (Fig. 3;
193 Extended Data Table 3). The soil CO_2 efflux response for the wet season was consistent with the
194 previously-reported 55% increase over 2-years of 3°C surface soil warming at this experiment
195 (including dry and wet seasons), which was shown to have arisen predominantly from increased
196 heterotrophic microbial activity[13]. Our observation of increased soil metabolic activity, indicated by
197 increased bacterial growth and enzyme activity with *in situ* soil warming, describes a further
198 acceleration of heterotrophic activity with warming. Enzymatic activity per unit of microbial biomass
199 increased for 7 out of 10 studied enzymes and markedly at +8°C *in situ* warming for enzymes that
200 degrade organic phosphorus, nitrogen, and carbon in phenolic and hemicellulose compounds (Fig. 2,
201 Extended Data Fig. 5–6). Collectively, the observed changes in process rates—of increased respiration,
202 growth and enzymatic activity per unit microbial biomass—corroborate our parallel findings that the

203 microbial community shifted towards favouring thermotolerant taxa that readily persist and even
204 increase in productivity under warmer conditions.
205
206 However, the predicted increase in soil CO_2 efflux based on the measured temperature sensitivity of
207 microbial respiration and growth in control soils (24–68% increase under 3–8°C warming; Fig. 3), was
208 substantially exceeded by the observed *in situ* increase in soil CO_2 efflux (78–337% under 3–8°C
209 warming; Fig. 3). Furthermore, the predicted CO_2 emission was only marginally higher when
210 accounting for adaptation of the microbial community to warmer conditions (measured T_{min} increase;
211 Fig. 2), resulting in a 25–77% increase under 3–8°C warming (Fig. 3). Importantly, we found no
212 evidence to suggest that the observed *in situ* increase in soil CO_2 emission occurred due to decreased
213 microbial metabolic efficiency, a common finding in short-term soil warming experiments where high
214 waste respiration exceeds growth[47]. Reduced metabolic efficiency is inconsistent with our previously
215 reported observation of no decrease in the size of the microbial biomass or in microbial CUE[48]
216 (measured using a stoichiometric method, see Supplementary Methods for discussion of this method
217 and its assumptions; Extended Data Fig. 5); a result in line with the independent observation of
218 increased microbial biomass under soil warming in tropical forest in Puerto Rico[49]. Similarly, we
219 cannot explain the augmented soil CO_2 emission by reference to accelerated substrate depletion, which
220 would also be expected to cause a decline in microbial biomass[50]. Indeed, microbial biomass remained
221 stable despite evidence for substrate depletion (decreased DOC and available P at 8°C warming;
222 Extended Data Fig. 5). Soil warming can also induce soil drying, potentially influencing CO_2 emission
223 and other community and process rate changes[8]. However, our study here was focused on the tropical
224 rainy season and despite lower moisture content in our +8°C treatment (Extended Data Fig. 5), we
225 expect this had negligible influence on our results because moisture remained non-limiting to
226 microbial activity. Finally, the augmented *in situ* soil CO_2 emission cannot be explained by increased
227 root respiration or substrate supply from root exudates, because by using root-partitioning cores we

found that warming had no effect on the root-derived soil CO_2 efflux[13]. Thus, we show that the temperature response of microbial community metabolism to warming—considered in models to be fundamental in explaining the long-term, and relatively large, response of soil C to climate warming[16,48]—only accounted for 23–32% of the observed *in situ* soil CO_2 emission.

In addition to biotic processes, our data point towards a further influence of abiotic processes in accelerating CO_2 emission at warmer temperatures. By using *ex situ* soil incubations across 2–40°C, we found that microbial growth declined at temperatures exceeding 34°C (Fig. 2); but enzyme activities increased—as did *in situ* soil CO_2 emissions (Figs. 2–3; Extended Data Fig. 6). These results can be explained by the effect of warming on the soil physico-chemical environment, including chemical oxidation/hydrolysis and desorption of mineral-stabilised organic matter and extracellular enzymes (Supplementary discussion)[51]. Clay-rich soils, such as those found at our tropical forest site, contain a large pool of stabilised C and inactive extracellular enzymes adsorbed to clay minerals.[52] At high temperatures desorption reaction rates can overtake adsorption reaction rates[53], thereby increasing the pools of active enzymes and labile C, and consequent CO_2 emissions. Consistent with a rapid increase in the pool of active enzymes driven by desorption, under warming we observed increased Q_{10} of V_{max} for four enzymes including phosphomonoesterase, β-xylanase and β-glucosidase (Fig. 2, Extended Data Fig. 5). A combination of these processes therefore resulted in increased enzyme activity that was uncoupled from growth (Fig. 2), contributing substantially to the observed CO_2 emissions that exceeded the predicted increase based on standard expectations from the observed temperature sensitivity and warm-adaptation response of the microbial community[15] (i.e. it was exceeded by 3.1–4.4 fold; Fig. 3).

In summary, our results show a progressive decline in tropical forest soil microbial diversity, especially for bacteria, and clear microbial community compositional shifts with warming (Fig. 1), occurring

alongside community growth-adaptation to temperature (Fig. 2) and resulting in further increased CO_2 emission (Fig. 3). This response of diversity declines under warming is contrary to observations from temperate forest warming studies[14,26]. Our data thus provide empirical support for the hypothesis that tropical soil communities are highly sensitive to warming and are consistent with independent evidence for deep evolutionary niche specialization in tropical soil microbes[30]. Further, we note that in view of the widespread evidence for intensive feedbacks among tropical soil microbial communities, plant diversity, and soil processes[25,41], declines in diversity may have substantial implications for overall tropical forest functioning, composition, and diversity in a warmer world. Alongside the decline in diversity observed in this experiment, the concurrent increased abundance of thermotolerant species resulted in a stable microbial biomass, accelerated enzymatic activity, and increased soil CO_2 emissions. This finding partially supports prior model-based projections showing increased C loss under climate warming this century due to adaptation of microbial growth[16]. However, our results go further by demonstrating that microbial models alone do not accurately predict the change in soil C emissions under warming in tropical ecosystems, especially at high temperatures where abiotic processes may accelerate C loss. Further study is urgently required to understand these combined biotic and abiotic controls on soil C in different tropical soils, the timescales of their effects, and the wider consequences of declines in soil microbial diversity for the functioning and composition of tropical forests in a warmer world.

METHODS

Site and experiment. The experiment is situated in seasonally moist lowland tropical forest on Barro Colorado Island, Panama. Within the experiment area (1 ha) the dominant tree species include *Anarcardium excelsum* and *Poulsenia armata;* a full census of tree and understory species composition in this forest is available for a nearby 50 ha forest plot in forest with similar soils, tree species and

278 demographic composition[54]. The soils are Inceptisols (Fine, isohyperthermic, Dystric Eutrudepts) that
279 are rich in clay (~54% profile-weighted clay concentration) and secondary metal oxides. The soils
280 developed on the volcanic facies of the Bohio Formation, a basaltic conglomerate of Oligocene age[55].
281 Inceptisols account for 14% of total land area in the tropics (Ultisols and Oxisols account for 20% and
282 23%, respectively)[56].
283
284 The SWELTR experiment consists of 10 circular plots (five paired plots 'warm' and 'control'). Each
285 plot measures 5 m diameter, with approximately 10 m between each plot-pair and a minimum of 20 m
286 between different plot-pairs. The experiment heats approximately 120 m^3 soil in total (5 plots x 5 m
287 diameter by 1.2 m depth). Temperature in the internal plot area (~3 m diameter) of each warmed plot
288 was maintained at 4°C above the temperature in each corresponding paired control plot, based on the
289 average temperature from 0–120 cm depth at the mid-radius points in each plot. For this study we
290 established subplots representing a high-temperature treatment, situated in a buffer-zone close to the
291 heating cable. We therefore had two subplots per plot, situated at approximately 10 cm and 1 m
292 distance from the one of the main heating rods, representing two different levels of warming. The
293 average warming for the low-warming subplot was 2.8°C and for the high-warming subplot was 7.9°C
294 (determined at 0–10 cm soil depth), based on the difference in temperature between control plots.
295 Thus, our study consisted of three treatments, soil at 26 ± 1°C ('Control'), 29 ± 2°C ('+3°C') and 34 ±
296 7°C ('+8°C'), providing a test of moderate (atmospheric warming with moderate fossil fuel emission
297 reduction) to extreme (atmospheric warming plus deforestation) predictions of warming for tropical
298 soils this century[5,31]. Further information on the plot design, thermostat control and power
299 specifications can be found in Nottingham *et al.* 2020[13].
300
301 ***Soil gas-exchange and partitioning.*** Soil CO_2 efflux was measured every week at four systematically
302 distributed locations within each plot from June 2018 to September 2018 (representing the 3°C surface

soil-warming treatment); and was measured twice-weekly at two systematically distributed locations within the high-warming subplot from August to September 2018 (representing the 8°C surface soil-warming treatment). Soil CO_2 efflux measurements were made using an infra-red gas analyser (IRGA Li-8100; LI-COR Biosciences, Nebraska, USA) and at the same time we measured soil temperature (using a HI98509 thermometer probe; Hanna Instruments, USA) and soil moisture (using a Thetaprobe; Delta-T, Cambridge, UK) at 0–20 cm soil depth for a random location immediately adjacent to each soil collar.

Soil sampling. Soil for this study was sampled during the wet season (June–Sept) in 2018. We sampled during the wet season to ensure that there was no moisture limitation to soil microbial activity and soil processes, and no difference in moisture limitation among treatments. Soil was sampled from 0–10 cm depth from the mineral horizon for each subplot and analysed for properties: total elements, available nutrients, exchangeable cations, microbial C, N and P and enzyme activities using standard procedures (see below and Supplementary Methods). We calculated microbial carbon-use-efficiency (CUE) using microbial CNP and enzyme activity data using a stoichiometric method (see Supplementary Methods). Soil samples were stored at −60ºC until DNA extraction (see below). All analyses were performed on replicate soil samples (n = 5).

Soil properties. Soil microbial biomass C and N were measured by fumigation-extraction[57,58] and extractable C and N were determined by fresh soil extraction in 0.5 M K_2SO_4. Extracts were analyzed for extractable organic C and N using a TOC-VCHN analyzer (Shimadzu, Columbia, MD). Microbial C and N were calculated as the difference between fumigated and unfumigated extracts and corrected for unrecovered biomass using a *k* factor of 0.45[59]. Microbial biomass P was determined by hexanol fumigation and extraction with anion-exchange membranes[60]. Extractable P was determined using unfumigated samples and microbial P was calculated as the difference between the fumigated and

unfumigated samples, with correction for unrecovered biomass using a k_p factor of 0.4[60]. Exchangeable cations were determined by extraction in 0.1 M $BaCl_2$ and detection by inductively coupled plasma-optical emission spectrometry (Optima 7300 DV; Perkin-Elmer Ltd, Shelton, CT, USA). Effective cation exchange capacity (ECEC) was calculated as the sum of the charge equivalents of Al, Ca, Fe, K, Mg, Mn and Na. Soil pH was determined in deionized water in a 1:2 soil to solution ratio. All analyses apart from total elements (C, N, P), cations, and pH were determined on fresh soils within 24 hours of sampling, and K_2SO_4 extracts within 6 h. All soil chemical properties are expressed on the basis of oven-dry equivalent soil (determined by drying at 105ºC for 24 hours).

DNA extraction, sequencing, and processing. DNA was extracted using the DNeasy Powersoil kit (Qiagen) and communities (bacterial and fungal) were amplified using a two-stage PCR protocol. For bacteria, we amplified the V4 hypervariable region of the 16S rRNA and for fungi we amplified the first internal transcribed spacer (ITS1) region of the rRNA operon (see SI methods for complete details). Libraries were sequenced on an Illumina MiSeq with 250bp paired end reads. Reads in the 16S rRNA and ITS data sets were first trimmed of forward and reverse primers. Based on visual inspection of read quality profiles, we removed the reverse reads from the 16S rRNA analysis due to poor quality. We then used DADA2[61] within the R environment (R Core Team, 2019) (v4.1.0) to filter and trim both datasets (based on quality profiles), error correct, dereplicate, and infer amplicon sequence variants (ASVs). We then merged pair-end reads (ITS only) and constructed sequence tables for both datasets. In the final step, we removed chimeras and assigned taxonomy (see Supplementary Methods for further detail).

Instantaneous temperature response of microbial growth and respiration. We used the instantaneous temperature response of microbial growth and respiration to: i) predict the effect of warming on *in situ* soil CO_2 emissions and ii) to determine the temperature adaptation of the bacterial community

following two years of *in situ* warming. For the former, we measured the instantaneous temperature response of respiration and bacterial and fungal growth for control soils only. For the latter, we measured the instantaneous temperature response of bacterial community growth for all warming treatments and controls; assuming the temperature adaptation respiration and fungal growth responded similarly as for bacterial growth, as found in tropical soils elsewhere[19,20]. To determine the temperature response of bacteria growth, we used the leucine incorporation method[19]; for the temperature response of fungal community growth, we used the acetate-in-ergosterol method[19]; for the temperature response of instantaneous respiration, we used incubation assays of 2 g soil in 20 ml vials for 24–140 hours at 10–30ºC and measurement of headspace CO_2. For full details, see Supplementary Methods and references therein.

Soil enzymes. Soil enzyme activity (V_{max}) was determined for ten enzymes involved in carbon and nutrient cycling, We used microplate assays to measure activity of α-glucosidase and β-glucosidase (degradation of α- and β-bonds in glucose), cellobiohydrolase (degradation of cellulose), β-xylanase (degradation of hemicellulose), *N*-acetyl β-glucosaminidase (degradation of *N*-glycosidic bonds), leucine aminopeptidase (degradation of leucine residues; N-rich amino acids), phenol oxidase (degradation of lignin via oxidation of phenols), phosphomonoesterase and phosphodiesterase (degradation of monoester- and diester-linked simple organic phosphates) and sulfatase (degradation of ester sulfates). For hydrolytic enzymes we used fluorometric assays with 100 μM methylumbelliferone (MU)-linked substrates, except for leucine aminopeptidase for which we used 7-amino-4-methylcoumarin (AMC) substrates. For oxidative enzymes (phenol oxidase) we used absorbance assays with L-3,4-dihydroxyphenylalanine (L-DOPA) substrates. For each soil sample, five replicate micro-plates were prepared and incubated at 2°C, 10°C, 22°C, 30°C and 40°C respectively, for calculation of the temperature sensitivity (Q_{10} of V_{max}) and determination of V_{max} at soil

temperature. Enzyme activities (V_{max}) are expressed on the basis activity at soil temperature per unit of microbial biomass C. To determine the Q_{10} of V_{max} we used:

$$Q_{10} = exp\ (10\ x\ k);\ where\ k = ln\frac{V_{max}}{t}$$

Where k is the exponential rate at which V_{max} increases with temperature (t). To calculate k (and thus Q_{10}) we used linear regression. See Supplementary Methods for detailed protocols.

Treatment effects on soil properties. To determine treatment effects on soil CO_2 emissions, soil moisture and temperature we used repeated measures ANOVA fitted by maximum likelihood (repeated measures model with time as random factor). To determine treatment effects (levels: control, +3ºC and +8ºC) on soil properties we used one-way ANOVA with post-hoc Tukey HSD tests. We used this approach for all soil properties, including enzyme V_{max} and the Q_{10} of V_{max} for each enzyme determined at soil temperature. Prior to analyses all data were tested for normality using a Shapiro-Wilk test and log-transformed where non-normally distributed.

Determination of T_{min} for respiration and growth and the predicted response of CO_2 efflux to in situ warming. In the square root model, the effect of temperature on activity is described by a quadratic increase up to an optimal temperature ($T_{opt,}$) and then a sharp decline[15,17], where the quadratic phase of the increase is constrained by the minimum temperature for activity (T_{min}, the y-intercept of the square root of activity plotted against temperature). The T_{min} of microbial activity was calculated using empirically defined microbial activity across the temperature range 4–28ºC (where the increase in the SQRT of activity is linear), according to the Ratkowsky (square root) equation[15,17]:

$$\sqrt{Activity} = a * (T - T_{min})$$

where T is the measurement temperature, T_{min} is the minimum temperature for activity (temperature where activity = 0) and *a* is empirically defined by the slope parameter from the square root of activity plotted against temperature; and where activity is either bacterial or fungal growth rates, or respiration. We determined T_{min} for each field replicate (n = 5 plots).

We then used the instantaneous temperature sensitivity of microbial activity (T_{min}) to model the CO_2 efflux response to warming, both with and without microbial community adaptation. Here we used T_{min} for bacteria growth only, because there was no significant difference in the T_{min} for bacterial growth (-1.39 ± 0.8) and respiration (0.3 ± 0.4) in control soils ($P = 0.1$). The T_{min} values for bacterial growth in control soils were also similar to those determined independently for two lowland tropical forests in Peru with similar mean annual temperature (-1.66 ± 0.7, -1.77 ± 1.0; MAT = 26.4°C)[19].

To model the CO_2 efflux response to warming we used the following equation:

$$\text{Predicted } CO_2 = [a * (T - T_{min})]^2$$

where T_{min} is for control soils. To model the CO_2 efflux response to warming following temperature-adaptation of microbial communities, we refitted the model using the T_{min} determined for bacterial growth in experimentally warmed soils for two years by 3°C and 8°C ('adapted' communities).

Microbial community analysis. To determine temperature treatment effects on alpha diversity of soil bacterial and fungal communities, we first applied general prevalence filtering using the R package PERFect (PERmutation Filtering test for microbiome data)[62] (v0.2.4). Here we used the function PERFect_sim with the alpha parameter set to 0.05 for the 16S rRNA data and 0.1 for the ITS data. We also applied two complementary methods of prevalence filtering to determine how filtering influenced alpha diversity estimates (see Supplementary Methods for complete details). We then calculated Hill numbers using the R package hilldiv[63] (v1.5.1), specifically Observed richness (q-value = 0), Shannon exponential (q-value = 1), and Simpson multiplicative inverse (q-value = 2). We used Shapiro-Wilk Normality test and Bartlett's test of Homogeneity of Variances to determine whether Hill numbers

were normally distributed. In cases where both p-values were greater than 0.05 (parametric data), we used ANOVA followed by Tukey post-hoc analysis to test for significance. For non-parametric data (cases where one or both p-values were less than 0.05), we instead used Kruskal-Wallis followed by Dunn test with Benjamini-Hochberg correction.

For soil bacterial and fungal beta diversity, we calculated distance matrices for the filtered data sets using unweighted and weighted UniFrac[64] for the 16S rRNA data and Jensen-Shannon Divergence and Bray-Curtis for the ITS data. To test for temperature treatment effects on beta diversity, we used the vegan package[65] (v2.5-7) to first calculate beta dispersion for the distance matrices (betadisper function), then perform a Permutation Test for Homogeneity of multivariate dispersions (permutest function), and finally run PERMANOVA (adonis function; assuming equal dispersion) or Analysis of Similarity (ANOSIM; where beta dispersion was significant).

To identify ASVs from the bacterial and fungal communities that were differentially abundant across temperature treatments, we used Indicator Species Analysis (ISA)[66] and linear discriminant analysis (LDA) effect size (LEfSe)[67]. Prior to differential abundance analysis, we applied PIME (Prevalence Interval for Microbiome Evaluation)[68] (v0.1.0) filtering to both complete datasets. PIME is a slightly more aggressive filtering tool specifically designed to work with data sets containing high variation among samples[68] — a pattern observed in the +8°C warming samples from the 16S rRNA data and all treatments from the ITS data (Extended Data Figs. 1c and 1f). PIME applies prevalence filtering on a per treatment basis and removes a substantial amount of within-group variation by eliminating low abundance ASVs in each treatment and retaining only those ASVs shared at the selected level of prevalence, within a given treatment[68]. Per the developer's recommendation, we first rarefied all samples to even depths (per sample: 16S rRNA = 25,088 reads, ITS = 9172 reads) and then split the data sets by predictor variable (temperature treatment) using the pime.split.by.variable function in R.

Next, we calculated all prevalence intervals from 5% to 95% (increments of 5%) with the function pime.prevalence and then used the function pime.best.prevalence to choose the best prevalence. The best prevalence interval was selected when the out-of-bag (OOB) error rate first reached zero or close to zero. The most prevalent ASVs (at the best prevalence interval) were retained from each split. Splits were then merged to obtain the final, PIME filtered data set. ISA was computed with the R package *labdsv*[69] (v2.0-1)—ASVs were considered an indicator of a treatment if they had a p-value less than or equal to 0.05. LEfSe analysis was performed within the R package microbiomeMarker[70] (v0.0.1) using the following parameters: pre-sample normalization of the sum of values set to $1e^{+06}$, lda_cutoff = 2, kw_cutoff = 0.5, and wilcoxon_cutoff = 0.5. We used anvi'o[71] (v7-dev) to visualize the distribution of PIME-filtered 16S rRNA ASVs represented by more than 100 total reads and PIME-filtered ITS ASVs represented by more than 50 reads. We then overlaid the results of the ISA and LEfSe analyses. Hierarchical clustering of ASVs was performed using Euclidean distance and Ward linkage against the ASV/sample abundance matrix while hierarchical clustering of samples was performed using Bray-Curtis distance and complete linkage.

To assess potential drivers of change in microbial community composition, we used three subsets of metadata to test correlations with community change; 1) environmental properties, 2) soil functional responses, and 3) temperature adaptive responses. For each of the three metadata subsets, we performed the following steps: i) use Shapiro-Wilk Normality Test to determine which metadata parameters are normally distributed; ii) use the R package bestNormalize[72] to find and execute the best normalization transformation for non-normally distributed parameters; iii) perform autocorrelation tests for all pair-wise comparisons; iv) remove autocorrelated parameters; v) run Mantel Tests to determine if any of the metadata subsets are significantly correlated with microbial community data; and vi) use the bioenv function (vegan package) to identify metadata parameters that are most strongly correlated with the community data. In last step, vii) we performed distance-based redundancy analysis

(dbRDA) using capscale from the vegan package. First, we ran rankindex (vegan) to select the best community dissimilarity index. Then, we ran capscale for distance-based redundancy analysis. Next, we used envfit (vegan) to fit environmental parameters onto ordinations. And finally, we selected all metadata parameters that were significant for bioenv (see above) and/or envfit analyses for plotting the ordinations and vector overlays. For full details including all references on community analyses methods, see Supplementary Methods.

References

1 Cavicchioli, R. *et al.* Scientists' warning to humanity: microorganisms and climate change. *Nature Reviews Microbiology* **17**, 569-586, doi:10.1038/s41579-019-0222-5 (2019).

2 Jackson, R. B. *et al.* The ecology of soil carbon: pools, vulnerabilities, and biotic and abiotic controls. *Annual Review of Ecology, Evolution, and Systematics* **48**, 419-445, doi:10.1146/annurev-ecolsys-112414-054234 (2017).

3 Pan, Y. *et al.* A large and persistent carbon sink in the world's forests. *Science* **333**, 988-993, doi:10.1126/science.1201609 (2011).

4 Myers, N., Mittermeier, R. A., Mittermeier, C. G., da Fonseca, G. A. B. & Kent, J. Biodiversity hotspots for conservation priorities. *Nature* **403**, 853-858, doi:Doi 10.1038/35002501 (2000).

5 IPCC. *Climate Change 2021: The Physical Science Basis. Contribution of Working Group I to the Sixth Assessment Report of the Intergovernmental Panel on Climate Change*. (Cambridge University Press, 2021).

6 Mora, C. *et al.* The projected timing of climate departure from recent variability. *Nature* **502**, 183, doi:Doi 10.1038/Nature12540 (2013).

7 Wood, T. E. *et al.* in *Ecosystem Consequences of Soil Warming: Microbes, Vegetation, Fauna and Soil Biogeochemistry* (ed J. Mohan) Ch. 14, 385-439 (Academic Press, 2019).

8 Davidson, E. A. & Janssens, I. A. Temperature sensitivity of soil carbon decomposition and feedbacks to climate change. *Nature* **440**, 165-173, doi:10.1038/nature04514 (2006).

9 van Gestel, N. *et al.* Predicting soil carbon loss with warming. *Nature* **554**, E4-E5, doi:10.1038/nature20150 (2018).

10 Melillo, J. M. *et al.* Long-term pattern and magnitude of soil carbon feedback to the climate system in a warming world. *Science* **358**, 101-104, doi:10.1126/science.aan2874 (2017).

11 Romero-Olivares, A. L., Allison, S. D. & Treseder, K. K. Soil microbes and their response to experimental warming over time: A meta-analysis of field studies. *Soil Biol Biochem* **107**, 32-40, doi:10.1016/j.soilbio.2016.12.026 (2017).

12 Anderson-Teixeira, K. J., Wang, M. M. H., McGarvey, J. C. & LeBauer, D. S. Carbon dynamics of mature and regrowth tropical forests derived from a pantropical database (TropForC-db). *Global Change Biol* **22**, 1690-1709, doi:10.1111/gcb.13226 (2016).

13 Nottingham, A. T., Meir, P., Velasquez, E. & Turner, B. L. Soil carbon loss by experimental warming in a tropical forest. *Nature* **584**, 234-237, doi:10.1038/s41586-020-2566-4 (2020).

14 DeAngelis, K. M. *et al.* Long-term forest soil warming alters microbial communities in temperate forest soils. *Front Microbiol* **6**, doi:ARTN 10410.3389/fmicb.2015.00104 (2015).
15 Bååth, E. Temperature sensitivity of soil microbial activity modeled by the square root equation as a unifying model to differentiate between direct temperature effects and microbial community adaptation. *Global Change Biol* **24**, 2850-2861, doi:10.1111/gcb.14285 (2018).
16 Wieder, W. R., Bonan, G. B. & Allison, S. D. Global soil carbon projections are improved by modelling microbial processes. *Nat Clim Change* **3**, 909-912, doi:Doi 10.1038/Nclimate1951 (2013).
17 Ratkowsky, D. A., Olley, J., Mcmeekin, T. A. & Ball, A. Relationship between temperature and growth-rate of bacterial cultures. *J Bacteriol* **149**, 1-5 (1982).
18 Rinnan, R., Rousk, J., Yergeau, E., Kowalchuk, G. A. & BÃ□Ã□Th, E. Temperature adaptation of soil bacterial communities along an Antarctic climate gradient: predicting responses to climate warming. *Global Change Biol* **15**, 2615-2625, doi:10.1111/j.1365-2486.2009.01959.x (2009).
19 Nottingham, A. T., Bååth, E., Reischke, S., Salinas, N. & Meir, P. Adaptation of soil microbial growth to temperature: using a tropical elevation gradient to predict future changes. *Global Change Biol*, doi:10.1111/gcb.14502 (2019).
20 Li, J. Q., Baath, E., Pei, J. M., Fang, C. M. & Nie, M. Temperature adaptation of soil microbial respiration in alpine, boreal and tropical soils: An application of the square root (Ratkowsky) model. *Global Change Biol* **27**, 1281-1292, doi:10.1111/gcb.15476 (2021).
21 Rousk, J., Frey, S. D. & Bååth, E. Temperature adaptation of bacterial communities in experimentally warmed forest soils. *Global Change Biol* **18**, 3252-3258, doi:10.1111/j.1365-2486.2012.02764.x (2012).
22 Nottingham, A. T. *et al.* Annual to decadal temperature adaptation of the soil bacterial community after translocation across an elevation gradient in the Andes. *Soil Biology and Biochemistry* **158**, 108217, doi:10.1016/j.soilbio.2021.108217 (2021).
23 Nottingham, A. T. *et al.* Microbial responses to warming enhance soil carbon loss following translocation across a tropical forest elevation gradient. *Ecol Lett* **22**, 1889-1899, doi:10.1111/ele.13379 (2019).
24 Donhauser, J., Niklaus, P. A., Rousk, J., Larose, C. & Frey, B. Temperatures beyond the community optimum promote the dominance of heat-adapted, fast growing and stress resistant bacteria in alpine soils. *Soil Biology and Biochemistry* **148**, 107873, doi:10.1016/j.soilbio.2020.107873 (2020).
25 Mangan, S. A. *et al.* Negative plant-soil feedback predicts tree-species relative abundance in a tropical forest. *Nature* **466**, 752-755, doi:10.1038/nature09273 (2010).
26 Pold, G., Melillo, J. M. & DeAngelis, K. M. Two decades of warming increases diversity of a potentially lignolytic bacterial community. *Front Microbiol* **6**, doi:ARTN 48010.3389/fmicb.2015.00480 (2015).
27 Zhou, J. Z. *et al.* Temperature mediates continental-scale diversity of microbes in forest soils. *Nat Commun* **7**, doi:ARTN 1208310.1038/ncomms12083 (2016).
28 Tedersoo, L. *et al.* Global diversity and geography of soil fungi. *Science* **346**, 1078 (2014).
29 Oliverio, A. M., Bradford, M. A. & Fierer, N. Identifying the microbial taxa that consistently respond to soil warming across time and space. *Global Change Biol* **23**, 2117-2129, doi:10.1111/gcb.13557 (2017).
30 Bahram, M. *et al.* Structure and function of the global topsoil microbiome. *Nature* **560**, 233, doi:10.1038/s41586-018-0386-6 (2018).
31 Spracklen, D. V., Baker, J. C. A., Garcia-Carreras, L. & Marsham, J. H. The effects of tropical vegetation on rainfall. *Annu Rev Env Resour* **43**, 193-218, doi:10.1146/annurev-environ-102017-030136 (2018).

32 Bradford, M. A. Thermal adaptation of decomposer communities in warming soils. *Front Microbiol* **4**, doi:10.3389/Fmicb.2013.00333 (2013).
33 Pietikäinen, J., Pettersson, M. & Bååth, E. Comparison of temperature effects on soil respiration and bacterial and fungal growth rates. *Fems Microbiol Ecol* **52**, 49-58, doi:10.1016/j.femsec.2004.10.002 (2005).
34 Mori, A. S. *et al.* Biodiversity–productivity relationships are key to nature-based climate solutions. *Nat Clim Change* **11**, 543-550, doi:10.1038/s41558-021-01062-1 (2021).
35 Delgado-Baquerizo, M. *et al.* Multiple elements of soil biodiversity drive ecosystem functions across biomes. *Nat Ecol Evol* **4**, 210-220, doi:10.1038/s41559-019-1084-y (2020).
36 Wagg, C., Bender, S. F., Widmer, F. & van der Heijden, M. G. A. Soil biodiversity and soil community composition determine ecosystem multifunctionality. *P Natl Acad Sci USA* **111**, 5266-5270, doi:10.1073/pnas.1320054111 (2014).
37 Nottingham, A. T. *et al.* Microbes follow Humboldt: temperature drives plant and soil microbial diversity patterns from the Amazon to the Andes. *Ecology* **99**, 2455-2466, doi:10.1002/ecy.2482 (2018).
38 Brown, J. H., Gillooly, J. F., Allen, A. P., Savage, V. M. & West, G. B. Toward a metabolic theory of ecology. *Ecology* **85**, 1771-1789, doi:10.1890/03-9000 (2004).
39 Brown, J. H. Why are there so many species in the tropics? *J Biogeogr* **41**, 8-22, doi:10.1111/jbi.12228 (2014).
40 LaManna, J. A. *et al.* Plant diversity increases with the strength of negative density dependence at the global scale. *Science* **356**, 1389-1392, doi:10.1126/science.aam5678 (2017).
41 Steidinger, B. S. *et al.* Climatic controls of decomposition drive the global biogeography of forest-tree symbioses. *Nature* **569**, 404, doi:10.1038/s41586-019-1128-0 (2019).
42 Lapebie, P., Lombard, V., Drula, E., Terrapon, N. & Henrissat, B. Bacteroidetes use thousands of enzyme combinations to break down glycans. *Nat Commun* **10**, doi:ARTN 204310.1038/s41467-019-10068-5 (2019).
43 Makhalanyane, T. P. *et al.* Microbial ecology of hot desert edaphic systems. *Fems Microbiol Rev* **39**, 203-221, doi:10.1093/femsre/fuu011 (2015).
44 Aydogan, E. L., Moser, G., Muller, C., Kampfer, P. & Glaeser, S. P. Long-Term Warming Shifts the Composition of Bacterial Communities in the Phyllosphere of Galium album in a Permanent Grassland Field-Experiment. *Front Microbiol* **9**, doi:ARTN 14410.3389/fmicb.2018.00144 (2018).
45 Hu, D. Y., Zang, Y., Mao, Y. J. & Gao, B. L. Identification of Molecular Markers That Are Specific to the Class Thermoleophilia. *Front Microbiol* **10**, doi:ARTN 118510.3389/fmicb.2019.01185 (2019).
46 Mohan, J. E. *et al.* Mycorrhizal fungi mediation of terrestrial ecosystem responses to global change: mini-review. *Fungal Ecol* **10**, 3-19, doi:10.1016/j.funeco.2014.01.005 (2014).
47 Manzoni, S., Taylor, P., Richter, A., Porporato, A. & Agren, G. I. Environmental and stoichiometric controls on microbial carbon-use efficiency in soils. *New Phytol* **196**, 79-91, doi:10.1111/j.1469-8137.2012.04225.x (2012).
48 Allison, S. D., Wallenstein, M. D. & Bradford, M. A. Soil-carbon response to warming dependent on microbial physiology. *Nat Geosci* **3**, 336-340, doi:10.1038/Ngeo846 (2010).
49 Reed, S. C. *et al.* Soil biogeochemical responses of a tropical forest to warming and hurricane disturbance. *Advances in Ecological Research* **62**, 225– 252 (2020).
50 Walker, T. W. N. *et al.* Microbial temperature sensitivity and biomass change explain soil carbon loss with warming. *Nat Clim Change* **8**, 885, doi:10.1038/s41558-018-0259-x (2018).
51 Kemmitt, S. J. *et al.* Mineralization of native soil organic matter is not regulated by the size, activity or composition of the soil microbial biomass—a new perspective. *Soil Biology and Biochemistry* **40**, 61-73, doi:10.1016/j.soilbio.2007.06.021 (2008).

52 Nannipieri, P., Trasar-Cepeda, C. & Dick, R. P. Soil enzyme activity: a brief history and biochemistry as a basis for appropriate interpretations and meta-analysis. *Biol Fert Soils* **54**, 11-19, doi:10.1007/s00374-017-1245-6 (2018).
53 Wallenstein, M., Allison, S., Ernakovich, J., Steinweg, J. M. & Sinsabaugh, R. in *Soil Enzymology* Vol. 22 *Soil Biology* (eds Girish Shukla & Ajit Varma) Ch. 13, 245-258 (Springer Berlin Heidelberg, 2011).
54 Condit, R., Perez, R., Lao, S., Aguilar, S. & Hubbell, S. P. Demographic trends and climate over 35 years in the Barro Colorado 50 ha plot. *For Ecosyst* **4**, doi:ARTN 1710.1186/s40663-017-0103-1 (2017).
55 Woodring, W. P. Geology of Barro Colorado Island. *Smithsonian Miscellaneous Collections* **135**, 1 – 39 (1958).
56 Sanchez, P. A. & Logan, T. J. Myths and Science About the Chemistry and Fertility of Soils in the Tropics. *Sssa Spec Publ* **29**, 35-46 (1992).
57 Brookes, P. C., Landman, A., Pruden, G. & Jenkinson, D. S. Chloroform fumigation and the release of soil-nitrogen - a rapid direct extraction method to measure microbial biomass nitrogen in soil. *Soil Biol Biochem* **17**, 837-842, doi:10.1016/0038-0717(85)90144-0 (1985).
58 Vance, E. D., Brookes, P. C. & Jenkinson, D. S. An extraction method for measuring soil microbial biomass-C. *Soil Biol Biochem* **19**, 703-707 (1987).
59 Jenkinson, D. S., Brookes, P. C. & Powlson, D. S. Measuring soil microbial biomass. *Soil Biol Biochem* **36**, 5-7, doi:10.1016/j.soilbio.2003.10.002 (2004).
60 Kouno, K., Tuchiya, Y. & Ando, T. Measurement of soil microbial biomass phosphorus by an anion-exchange membrane method. *Soil Biol Biochem* **27**, 1353-1357 (1995).
61 Callahan, B. J. *et al.* DADA2: High-resolution sample inference from Illumina amplicon data. *Nat Methods* **13**, 581-583, doi:10.1038/nmeth.3869 (2016).
62 Smirnova, E., Huzurbazar, S. & Jafari, F. PERFect: PERmutation Filtering test for microbiome data. *Biostatistics* **20**, 615-631, doi:10.1093/biostatistics/kxy020 (2019).
63 Alberdi, A. & Gilbert, M. T. P. hilldiv: an R package for the integral analysis of diversity based on Hill numbers. *bioRxiv*, 545665, doi:10.1101/545665 (2019).
64 Lozupone, C., Lladser, M. E., Knights, D., Stombaugh, J. & Knight, R. UniFrac: an effective distance metric for microbial community comparison. *Isme J* **5**, 169-172, doi:10.1038/ismej.2010.133 (2011).
65 Vegan: Community Ecology Package (R Package Version 2 (0), 2012).
66 Dufrene, M. & Legendre, P. Species assemblages and indicator species: The need for a flexible asymmetrical approach. *Ecological Monographs* **67**, 345-366, doi:10.1890/0012-9615(1997)067[0345:Saaist]2.0.Co;2 (1997).
67 Segata, N. *et al.* Metagenomic biomarker discovery and explanation. *Genome Biol* **12**, doi:ARTN R6010.1186/gb-2011-12-6-r60 (2011).
68 Roesch, L. F. W. *et al.* pime: A package for discovery of novel differences among microbial communities. *Mol Ecol Resour* **20**, 415-428, doi:10.1111/1755-0998.13116 (2020).
69 labdsv: Ordination and multivariate analysis for ecology (R package, 2017).
70 microbiomeMarker: microbiome biomarker analysis (2020).
71 Eren, A. M. *et al.* Anvi'o: an advanced analysis and visualization platform for 'omics data. *Peerj* **3**, e1319, doi:10.7717/peerj.1319 (2015).
72 Peterson, R. A. & Cavanaugh, J. E. Ordered quantile normalization: a semiparametric transformation built for the cross-validation era. *J Appl Stat* **47**, 2312-2327, doi:10.1080/02664763.2019.1630372 (2020).

End notes

Acknowledgements | This study was supported by three fellowships to ATN, a European Union Marie-Curie Fellowship FP7-2012-329360, a STRI Tupper Fellowship and a UK NERC grant NE/T012226. Further support came from a UK NERC grant NE/K01627X/1, an ANU Biology Innovation grant to PM and Simons Foundation grant No. 429440 to W. Wcislo, STRI, and support from the U.S. Department of Agriculture (USDA), Agricultural Research Service to KB. We thank Ben Turner for his contribution to SWELTR during its initial phase of operation. For their support we further thank Oris Acevado, Dayana Agudo, Aleksandra Bielnicka, Gloria Broders, Melissa Cano, David Dominguez, Milton Garcia, Matthew Larsen, Julio Rodriguez, Hubert Szczygiel, Irene Torres, Esther Velasquez, William Wcislo, Klaus Winter and Joe Wright.

Author contributions | ATN conceived the study. ATN, JJS, MM, JP, EB, KB and KS performed the study. ATN and JJS analysed the data. ATN wrote the paper with input from JJS, EB, KS, KB and PM.

Author Information | The authors declare no competing financial interests. Mention of trade names or commercial products in this publication is solely for the purpose of providing specific information and does not imply recommendation or endorsement by the USDA. The USDA is an equal opportunity provider and employer. Reprints and permissions information is available at www.nature.com/reprints. Correspondence and requests for materials should be addressed to A.T.N. (A.Nottingham@leeds.ac.uk).

Data availability

Trimmed (primers removed) sequence data generated in this study are deposited in the European Nucleotide Archive (ENA) under Project Accession number PRJEB45074 (ERP129199), sample accession numbers ERS6485270–ERS6485284 (16S rRNA) and sample accession numbers ERS6485285– ERS6485299 (ITS). Raw fastq files can be accessed through the Smithsonian figshare, at https://doi.org/10.25573/data.14686665 (16S rRNA) and https://doi.org/10.25573/data.14686755 (ITS). Related data and data products for individual analysis workflows are available through the Smithsonian figshare under the collection https://doi.org/XXXXX.[†]

Code availability

[†] A figshare DOI for the collection containing related data & data products will be generated upon final manuscript acceptance.

All code, reproducible workflows, and further information on data availability can be found on the project website at https://sweltr.github.io/high-temp/. The code embedded in the website is available on GitHub [https://github.com/sweltr/high-temp/] in R Markdown format. The version of code used in this study is archived under SWELTR Workflows v1.0 (REF) [https://github.com/sweltr/high-temp/releases/tag/v1.0], DOI identifier, https://doi.org/XXX/zenodo.XXXXXX.‡

Extended Data is available for this manuscript, including the following:

Extended Data: Tables 1 to 3

Extended Data: Figs. 1 to 6

Supplementary Information is available for this manuscript, including the following:

Supplementary Methods

Supplementary Discussion

‡ A workflow version number (GitHub) and a DOI for the code (generated through Zenodo) will both be generated upon final manuscript acceptance.

Figures

Figure 1 | Microbial diversity decline and community change under 3°C and 8°C *in situ* soil warming in lowland tropical forest. Two years of soil warming caused significant decreases in (**a**) bacterial and (**b**) fungal diversity, determined by 16S rRNA and ITS sequencing, respectively. Data from the PIME filtered data sets for controls (blue), 3°C warming (green) and 8°C warming (red). Hierarchical clustering of ASVs (top dendrograms) based on Euclidean distance and Ward linkage. Hierarchical clustering of samples (right dendrograms) based on Bray-Curtis distance and complete linkage. Each vertical line in the main plot represents a unique ASV, where colour intensity indicates the log-normalized abundance, and no colour indicates an ASV that was either not detected or removed during prevalence filtering. The coloured bars below indicate ASVs that were enriched in different temperature treatments as determined by either Indicator Species Analysis (IndVal) or Linear discriminant analysis Effect Size (LEfSe). Additional data for each sample are presented in the plots on the right. Diversity estimates charts show the total number of reads, observed richness, Shannon exponential index, and Inverse Simpson index. Taxonomic profiles show the proportion of major classes (16S rRNA data) or orders (ITS data).

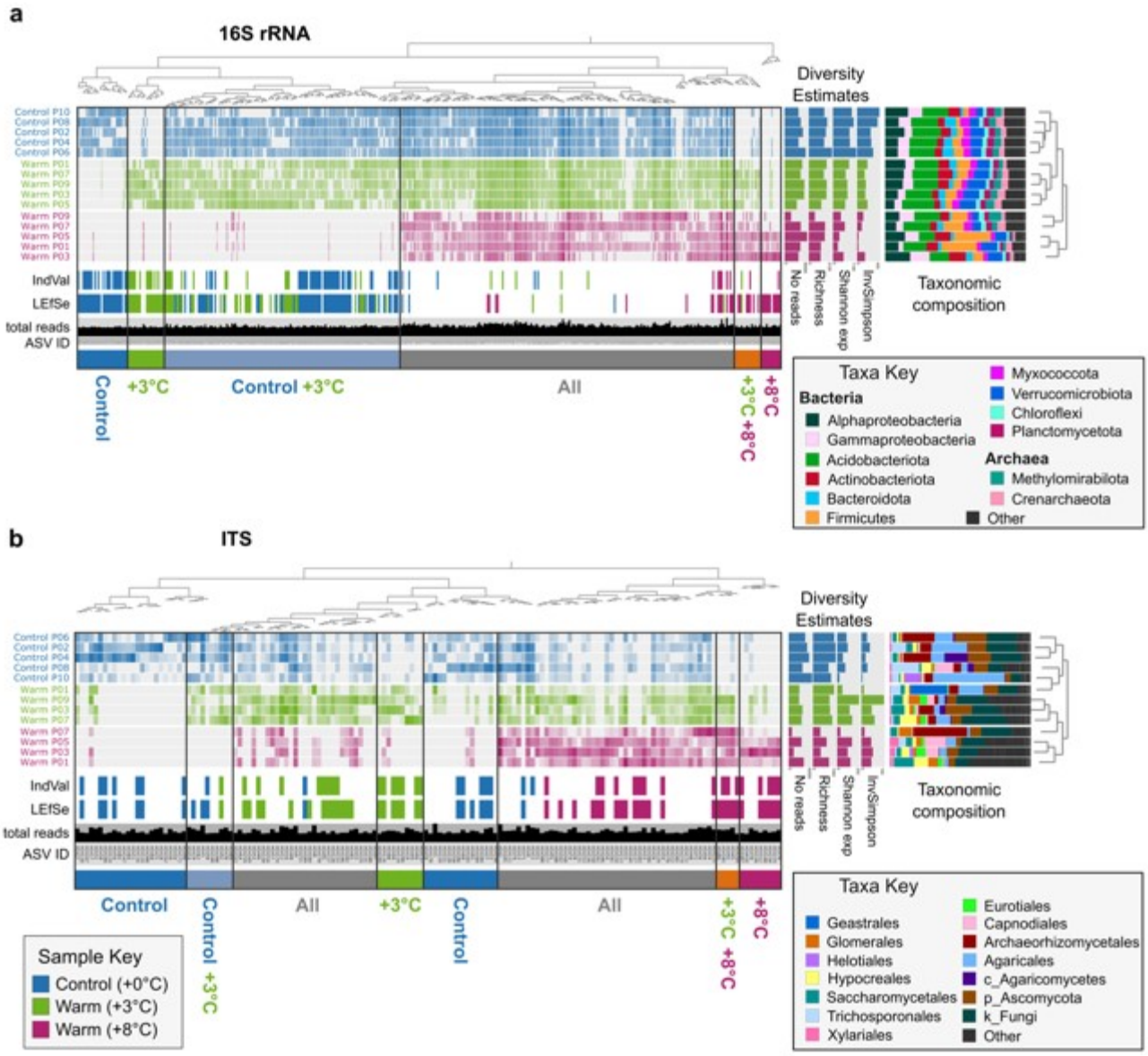

Figure 2 | The response of (a–b) microbial growth and (c–d) enzyme activity to 3°C and 8°C soil warming, and (e) the relationship between the temperature response of growth and activity with microbial community changes. (**a–b**) Microbial growth was determined for bacteria for each treatment using Leu-incorporation incubation assays across a temperature range of 4–40°C. The minimum temperature for growth (T_{min}) increased with warming (see **b**), but growth declined at high temperatures (>30–34°C; see lighter shaded points in (a); these data were not used for the linear model to determine T_{min}). **(c)** Activities were determined for 10 enzymes (ß-xylanase shown here, six others responded similarly; see SI) across an incubation temperature range of 4–40°C. The maximum potential activity—at soil temperature per unit microbial C—increased with warming for 7 out of 10 enzymes (see **d**) and increased across high temperature ranges (to 40°C) illustrating a decoupling of growth and activity above 30°C. (**e**) The microbial community composition change was related to the temperature response of growth (T_{min}) and of enzyme activities (Q_{10} of V_{max}) for **i**) bacteria and **ii**) fungi. Bacterial growth and enzyme activity are plotted using a linear transformation (square root). Microbial community composition change estimated using Distance-based Redundancy Analysis (db-RDA) based on Bray-Curtis dissimilarity; see Extended Data (Table 2, Fig. 4) for relationships between community composition change and other soil properties. All analyses are for n = 5 plots.

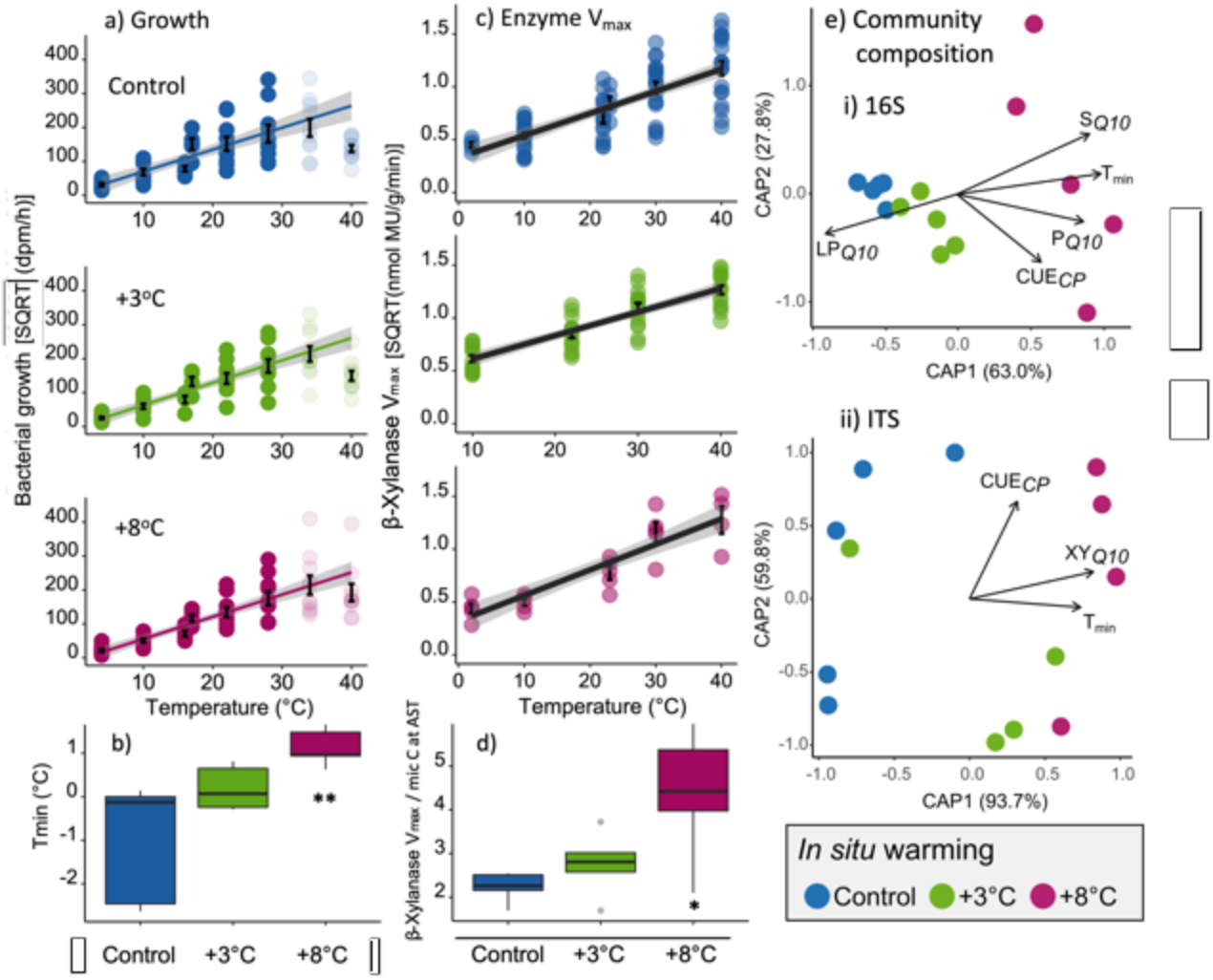

Figure 3 | The response of soil CO_2 efflux to *in situ* warming by 3 to 8°C is greater than the increase predicted by the temperature response of microbial respiration and growth (a). Data points are measurements of soil CO_2 efflux from control (blue), 3°C warming (green) and 8°C warming (red). The response of CO_2 emission to temperature was described by a square root function ('Observed' line; $CO_2 = 1.9 \times T^2 - 45$; $R^2 = 0.68$, $P < 0.001$, F = 556). The modelled CO_2 efflux responses ('Predicted' lines) are based on measured T_{min} at ambient temperature (blue dash line = no adaptation; $CO_2 = 1.21 \times T^2 - 0.17$; $R^2 = 0.87$, $P < 0.001$, F = 124) and T_{min} change after two years of warming indicating community adaptation (green dash line = 3°C adaptation, $CO_2 = 1.24 \times T^2 - 0.18$; $R^2 = 0.87$, $P < 0.001$, F = 118; and red dash line = 8°C adaptation, $CO_2 = 1.25 \times T^2 - 0.20$; $R^2 = 0.86$, $P < 0.001$, F = 111). The box plots show the treatment effects on (**b**) soil CO_2 efflux and (**c**) soil temperature (repeated measures ANOVA; ** $P < 0.01$; *** $P < 0.001$). The centre line of each box plot represents the median, the lower and upper hinges represent the first and third quartiles and whiskers represent + 1.5 the interquartile range; the dashed lines represent means. The soil temperature and soil CO_2 efflux by treatment was, for controls: 26 ± 1 °C and 4.74 ± 0.25 µmol CO_2 m^{-2} s^{-1}, 3°C warming: 29 ± 2°C and 8.42 ± 0.44 µmol CO_2 m^{-2} s^{-1}, 8°C warming: 34 ± 7°C and 15.98 ± 1.68 µmol CO_2 m^{-2} s^{-1}) (mean ± one standard error, n = 5 plots).